SANDIA REPORT

SAND2014-18696
Unlimited Release
Printed October 2014

Rheological and Mechanical Property Measurements of PMDI foam at Elevated Temperatures

Martin B. Nemer, Carlton F. Brooks, Bion Shelden, Melissa M. Soehnel,
David A. Barringer

Prepared by
Sandia National Laboratories
Albuquerque, New Mexico 87185 and Livermore, California 94550

Sandia National Laboratories is a multi-program laboratory managed and operated by Sandia Corporation, a wholly owned subsidiary of Lockheed Martin Corporation, for the U.S. Department of Energy's National Nuclear Security Administration under contract DE-AC04-94AL85000.

Issued by Sandia National Laboratories, operated for the United States Department of Energy by Sandia Corporation.

Available to DOE and DOE contractors from
U.S. Department of Energy
Office of Scientific and Technical Information
P.O. Box 62
Oak Ridge, TN 37831

Telephone: (865) 576-8401
Facsimile: (865) 576-5728
E-Mail: reports@adonis.osti.gov
Online ordering: http://www.osti.gov/bridge

Available to the public from
U.S. Department of Commerce
National Technical Information Service
5285 Port Royal Rd.
Springfield, VA 22161

Telephone: (800) 553-6847
Facsimile: (703) 605-6900
E-Mail: orders@ntis.fedworld.gov
Online order: http://www.ntis.gov/help/ordermethods.asp?loc=7-4-0#online

SAND2014-18696
Unlimited Release
Printed October 2014

Rheological and Mechanical Measurements of PMDI foam

Martin Bernard Nemer, Carlton F. Brooks, Bion Shelden, Melissa M. Soehnel,
and David A. Barringer
Thermal and Fluid Sciences
Sandia National Laboratories
P.O. Box 5800
Albuquerque, New Mexico 87185-MS0346

Abstract

A study was undertaken to determine the viscosity of liquefied 20 lb/ft^3 poly methylene diisocyanate (PMDI) foam and the stress required to puncture solid PMDI foam at elevated temperatures. For the rheological measurements the foam was a priori liquefied in a pressure vessel such that the volatiles were not lost in the liquefaction process. The viscosity of the liquefied PMDI foam was found to be Newtonian with a power law dependence on temperature $\log_{10}(\mu/\text{Pa s}) = 20.6 - 9.5 \log_{10}(T/°C)$ for temperatures below 170 °C. Above 170 °C, the viscosity was in the range of 0.3 Pa s which is close to the lower measurement limit (≈ 0.1 Pa s) of the pressurized rheometer. The mechanical pressure required to break through 20lb/ft^3 foam was 500-800 psi at temperatures from room temperature up to 180 °C. The mechanical pressure required to break through 10 lb/ft^3 was 170-300 psi at temperatures from room temperature up to 180 °C. We have not been able to cause gas to break through the 20 lb/ft^3 PMDI foam at gas pressures up to 100 psi.

ACKNOWLEDGMENTS

The authors would like to acknowledge helpful discussions with Anne Grillet for teaching the authors how to properly make rheological measurements and for helping the authors understand the limitations of the rheometric instrumentation. The authors would like to acknowledge Lindsey Hughes for teaching the authors how to make PMDI foam rods and for help setting up the high-pressure equipment. The authors would like to thank Ryan Keedy for his careful technical review of this SAND report.

CONTENTS

FIGURES

TABLES

NOMENCLATURE

dB	decibel
DOE	Department of Energy
EGA	Evolved Gas Analysis
FIC	Foam-in-a-Can
GC/MS	Gas Chromatography/Mass Spectrometry
GPC	Gel Permeation Chromatography
HTHP	High Temperature High Pressure
PMDI	poly methylene-4,4’ diphenyl diisocyanate
SNL	Sandia National Laboratories
TDI	poly toluene diisocyanate
TGA	Thermal Gravimetric Analysis

1. INTRODUCTION

When polymers are exposed to a source of heat, such as fire, they undergo both physical and chemical changes. Sandia's work in the area of polyurethane foams in fire environments began in the 1990's (Hobbs, et al., 1999), however work in this area goes back to at least the 1970's (Pfeiffer and Steger, 1978). Many researchers have performed thermal-gravimetric-analysis (TGA) coupled with evolved gas analysis (EGA) on toluene and methylene based polyurethane foams (Allan, et al., 2013, Bilbao, et al., 1996, Erickson, 2006, Erickson, 2007, Hobbs, et al., 2001b, Hobbs, et al., 2001a, Jiao, et al., 2013, Kim, et al., 2012, Li, et al., 2006, Wang, et al., 2014). Other researchers have examined decomposition of non-foamed types of polyurethanes (Chattopadhyay and Webster, 2009, Hentschel and Munstedt, 2001, Herrera, et al., 2002). In nitrogen or inert gas, it is generally recognized that breakdown of the polyurethane foam begins at ≈ 170 °C, and is mostly complete by ≈ 300 °C (Bilbao, et al., 1996). The decomposition products are generally recognized to be shorter chained diisocyanates, polyols, amines (aniline in particular), carbon dioxide, and short chained aliphatics (Bilbao, et al., 1996). The moles of gas evolved during liquefaction of polyurethane foams at temperatures below 350 °C is mostly CO_2 and water (Kim, et al., 2012, Allan, et al., 2013, Erickson, 2006). Most of the above referenced studies have focused on the decomposition products in the gas phase, under unconfined or partially confined conditions. Far less work has been performed to determine the composition of the gas phase under full confinement and/or the composition of the resulting liquefied phase. Yang (1986) performed gel-permeation-chromatography (GPC) of the decomposed/liquefied phase for a polyurethane material that is similar to our PMDI foams, after heating to 250 °C; the resolved peaks had lengths from 6 – 10 monomeric units of the original polymer.

In this work we focus on poly methylene-4,4'diphenyl diisocyanate (PMDI, also known as MDI) foam. Methodology was developed for liquefying PMDI foam without significant loss of the volatile components and subsequently measuring the rheology of the liquefied foam within a high-temperature high-pressure (HTHP) rheometer vessel. We also attempted to measure the gas breakthrough and permeability and mechanical breakthrough of 10lb/ft^3 and 20lb/ft^3 PMDI foam.

2. EXPERIMENTAL METHODOLOGY

2.1 Production of PMDI foam

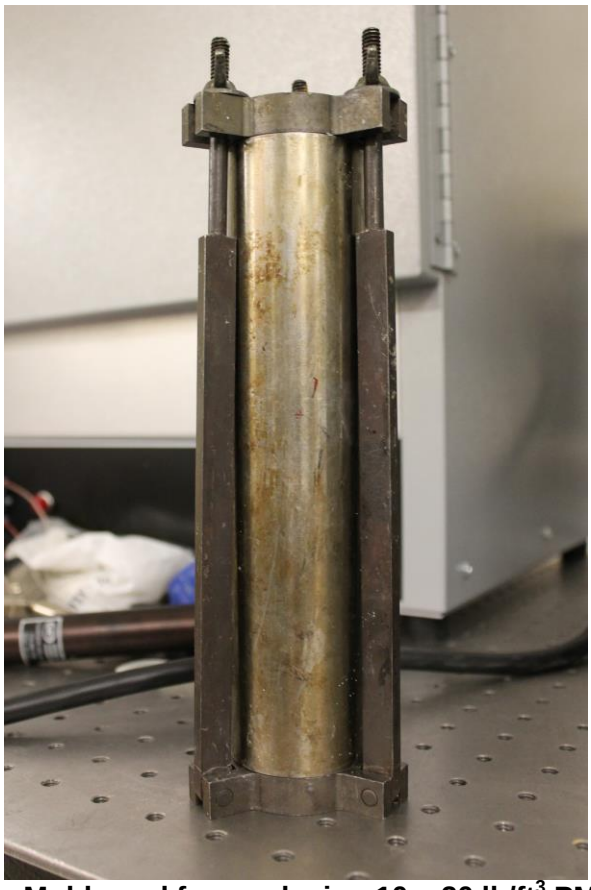

Figure 1. Mold used for producing 10 – 20 lb/ft^3 PMDI rods.

Figure 2. Image of virgin 20 lb/ft^3 PMDI rod, 8" long by 1.125" in diameter.

Ten and 20 lb/ft^3 structural PMDI foam rods were prepared using structural PMDI obtained from Honeywell (FM&T). For both 10 lb/ft^3 and 20 lb/ft^3, Honeywell structural PMDI foam -10 T (T component) and -10 R (R component) were used, which is intended for producing 10 - 20lb/ft^3 foam.

The recipe for producing the foam rods was as follows. The mold (Figure 1) was coated with mold release (Chem Trend, Permamold 929TO) and then pre-heated in an oven to 40 °C for at

least one hour. For 20 lb/ft^3 foam, 16.7g of the R component and 38.3g of the T component were mixed for 45 seconds in a disposable 500mL beaker. Next 42g were poured into the mold which was sealed and returned to the 40 °C oven for at least one hour. For producing the 10lb/ft^3 foam, 10.6g of the R component and 24.4g of the T component were mixed in a 500mL disposable beaker for 45 seconds. Next 24g of the mixture were poured into the mold which was sealed and returned to the 40 °C oven for at least one hour. After one hour the mold was cooled until it could be handled by touch and then the rod was hammered out of the mold using a metal punch. An image of the resulting rod is shown in Figure 2.

The mold used for the 10lb/ft^3 and 20lb/ft^3 is 8 inches long by 1.125 inches in diameter. Thus each rod had a volume of 130 cm^3. The 20 lb/ft^3 and 10 lb/ft^3 PMDI foam rods used for the mechanical breakthrough tests (Sections 2.4 and 3.4) were measured for density. The actual density of the 20 lb/ft^3 foam was 20.8 ± 0.5 lb/ft^3. The actual density of the 10 lb/ft^3 foam was 11.5 ± 0.2 lb/ft^3. These densities should be representative of all of the work on PMDI given herein.

2.2 Liquefaction of PMDI foam

Figure 3. Image of Autoclave Engineers pressure vessel used to liquefy PMDI foam.

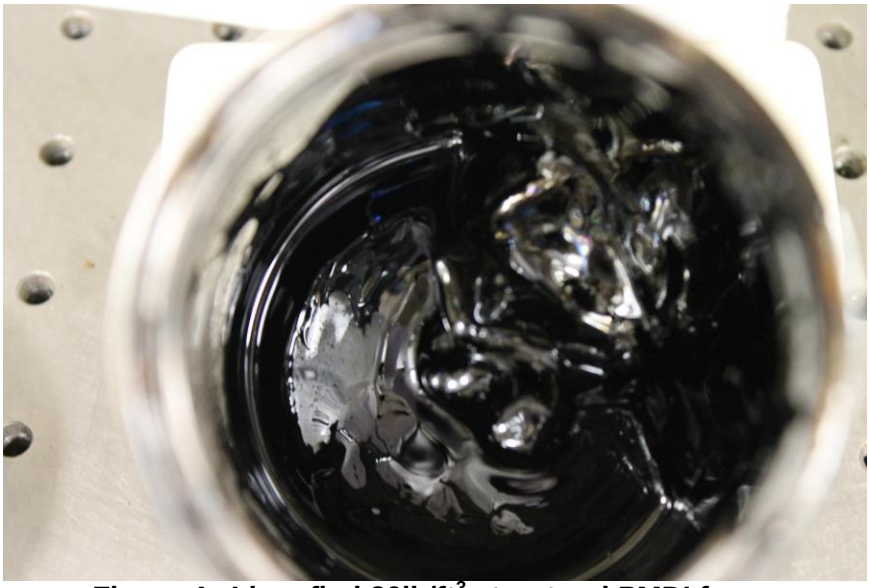

Figure 4. Liquefied 20lb/ft^3 structural PMDI foam.

Liquefaction of PMDI foam was accomplished using an Autoclave Engineers 1L Hastelloy C-276 pressure vessel, model H100HCA0131X000X000021M1101X, capable of temperatures up to 500 °C, and pressures up to 5000 psi. This vessel was purchased for the purpose of liquefying PMDI and TDI foams, measuring off-gas products at high temperatures, and determining vapor pressures of decomposition products. The vessel is shown in Figure 3. Rods of 20lb/ft^3 structural PMDI (Section 2.1) were placed into the vessel, the vessel was sealed, and inert gas was flowed through the vessel for at least 30 minutes to remove any oxygen. A headspace pressure of 600 psi of inert gas (He or N_2) was placed on the vessel to keep oxygen out. Two rods at a time were cooked at temperatures up to 325 °C for one hour, although the vessel takes several hours to cool back to room temperature. This temperature ceiling was chosen because it was believed to be the lowest temperature at which liquefaction could occur; we now know that liquefaction can occur at significantly lower temperatures (225 °C, and perhaps as low as 170 °C, see Bilbao, et al., 1996). Vessel temperature was measured via a thermocouple within a thermo well, which is located several inches off the bottom of the vessel. The vessel wall was heated to higher temperatures (~ 425 °C) in order to maintain the internal temp of 325 °C. Once the vessel was cool, the vessel could be vented, opened and the product removed. The resulting product is shown in Figure 4. The liquefied foam is jet black and shows specular reflectivity. The liquefied foam is tacky but does not flow at room temperature.

2.3 Rheology of liquefied PMDI foam

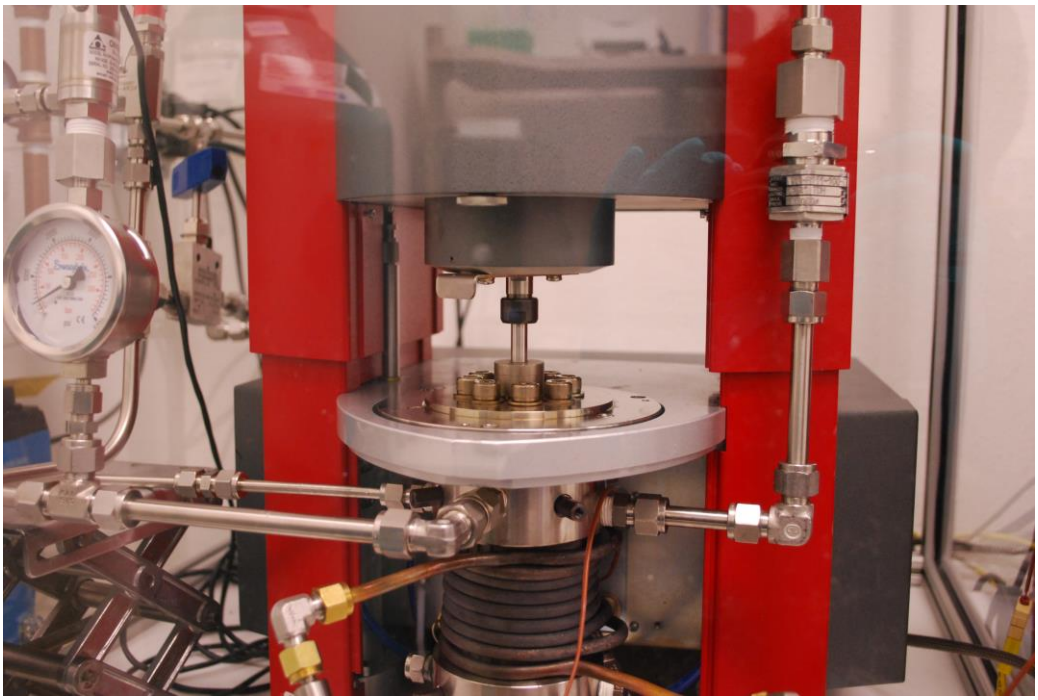

Figure 5. High Pressure High Temperature Rheometer

Rheology of the liquefied foam was measured in a high-temperature (up to 425 °C) high-pressure (up to 4000 psi) ATS Rheosystems rheometer vessel shown in Figure 5. The sealed vessel transmits torque through a magnetic coupling with the ATS Rheosystems rheometer head. The geometry of the rheometer vessel is Couette flow. The inner cylinder (bob) rotates with the rheometer head through the magnetic coupling. Because of the large mass of the inner cylinder and because of the magnetic coupling, this system is only capable of steady-state measurements; oscillatory measurements were not possible.

To fill the pressurized rheometer vessel, the rheometer vessel and the liquefied PMDI foam (produced in the Autoclave vessel, see Section 2.2) were heated to ~ 90 °C, open to the atmosphere, at which point the liquefied PMDI foam (Figure 4) is able to flow. The vessel was then filled until the bob was completely covered by the black tar-like material. Then the vessel was sealed. An inert gas (He or N_2) was flowed through the vessel before heating it to the desired temperature. A headspace pressure of 500 psi was maintained to keep oxygen out of the vessel.

2.4 Mechanical pressure breakthrough of PMDI foam

Figure 6. Texture Technologies texture analyzer.

The mechanical breakthrough strength of virgin PMDI foam was measured using a Texture Technologies Corp. TA XTplus texture analyzer. This instrument consists a rigid metal probe connected to a load cell which moves downward into and through a sample at a given velocity, while measuring the force required to maintain that velocity. In tests performed to date, we have used a 2mm diameter probe; other probes will be used in future work. PMDI rods (20lb/ft^3 and 10lb/ft^3), as shown in Figure 2, were sliced into ¼″-thick discs, which were placed in a circular counter bore within a large aluminum plate shown in Figure 6. The aluminum plate was heated via a hot plate, with a thermocouple attached to the plate to measure and record the sample/plate temperature. The foam disc was held at temperature for a specified amount of time (hold time) before beginning the mechanical test.

2.5 Gas pressure breakthrough of PMDI foam

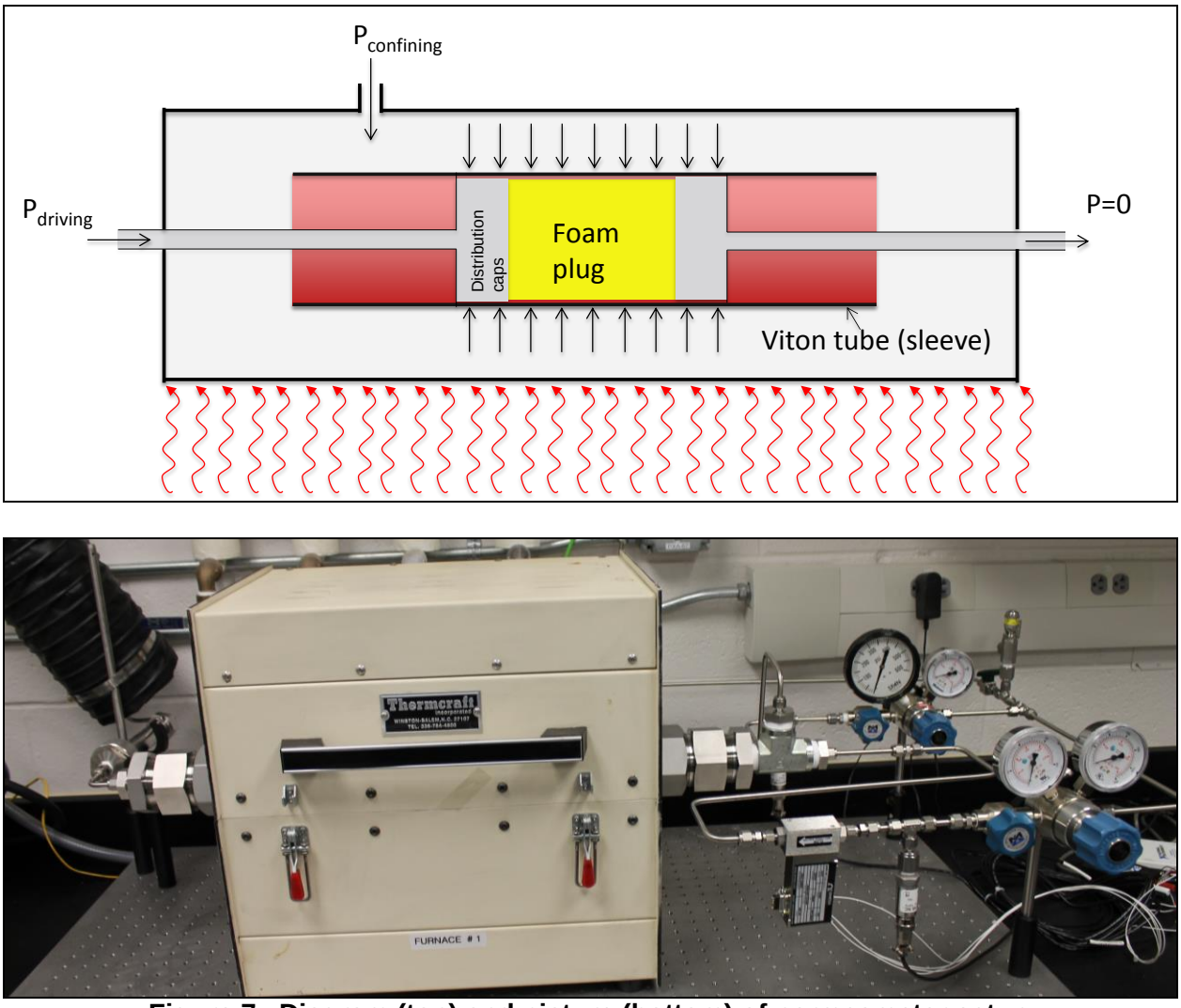

Figure 7. Diagram (top) and picture (bottom) of permeameter setup

Experiments were designed to obtain the gas-pressure required to cause gas to break through the closed cell structure of the PMDI foam, and to obtain the resulting permeability of the gas-fractured (hydrofractured) material. The system, shown in Figure 7, consists of an inner Viton cylindrical sleeve in which is placed a foam sample sandwiched between two metal distribution caps. One distribution cap is plumbed to an inert gas at elevated pressure, $P_{driving}$. The other distribution cap is open on the far end to atmospheric pressure. A separate elevated gas pressure, $P_{confining}$, is applied to the annulus between the Viton sleeve and an outer confining cylinder to maintain strong contact of the sleeve with the distribution caps and the foam plug. This ensures that gas flow is forced to go through the foam plug and not around it. The flow rate through the sample is monitored by a digital mass flow meter, and pressures $P_{driving}$ and $P_{confining}$ are controlled via regulators. The cylinder containing the Viton sleeve, foam plug, and distribution caps are heated via a tube furnace capable of 1100 °C. The Viton sleeve can withstand 300 °C, although copper sleeves may be used for higher temperatures in future work on materials that

liquefy at higher temperatures. The highest gas pressures available in the current setup are 500 psi.

3. RESULTS

3.1 Liquefaction of 20lb/ft^3 structural PMDI foam

3.1.1. Pressure response during liquefaction

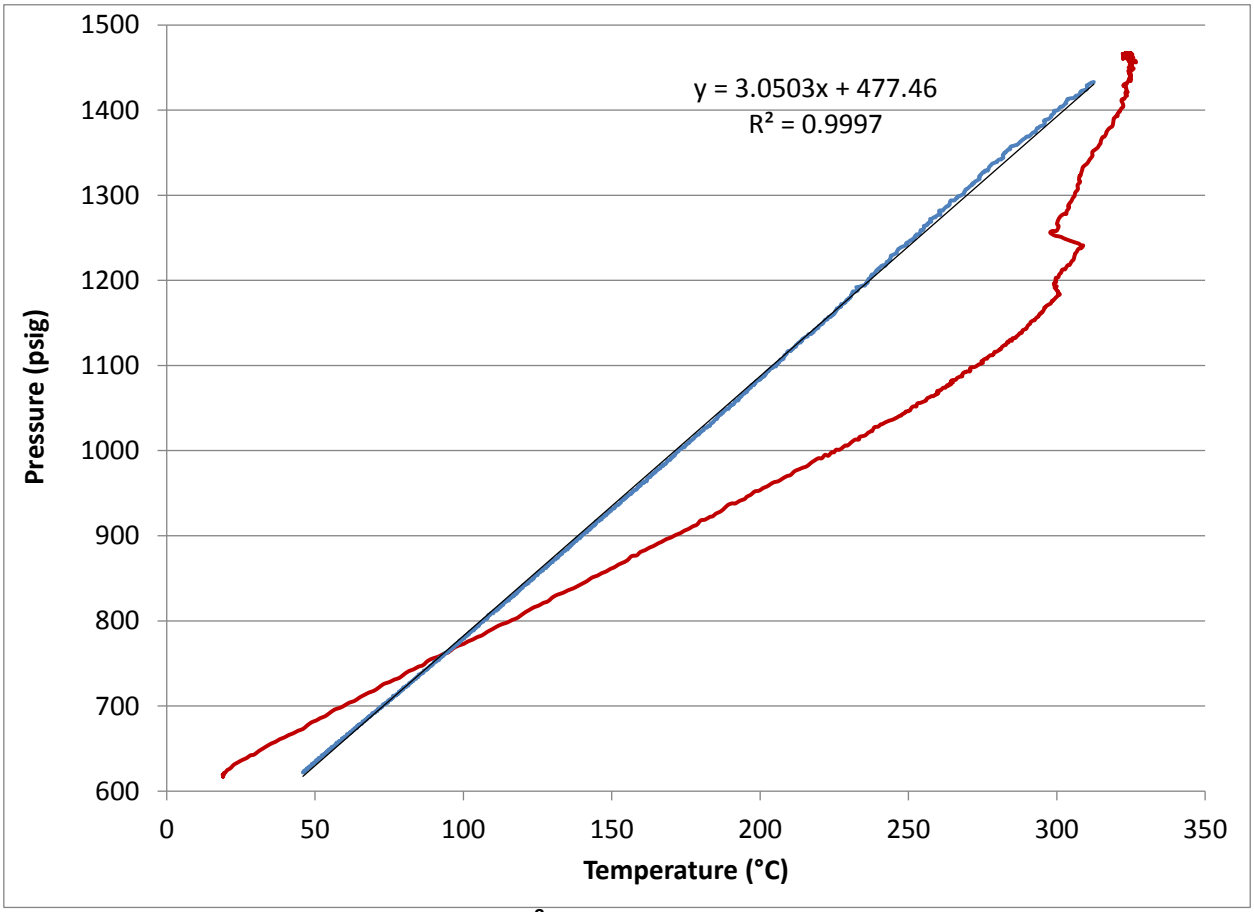

Figure 8. Pressure data from a 20lb/ft^3 structural PMDI liquefaction. The red curve is the pressure during active heating, the blue curve is the pressure during cooling.

During the 1/17/2013 liquefaction run, 86.4g of 20lb/ft^3 structural PMDI was loaded into the pressure vessel. The liquefied material removed from the pressure vessel weighed 62.9g. Thus at most 23.5g grams went into the gas phase, recognizing that some liquefied material could not be removed from the pressure vessel.

During liquefaction, the pressure in the Autoclave Engineers pressure vessel is continuously monitored and recorded. Figure 8 shows the pressure during the heating portion of the cycle (red curve) and the pressure during cooling (blue curve). The initial pressure is 619 psig. At ~ 300 °C the pressure rises from 1185 psi to 1465 psig, corresponding to a jump in pressure of 280 psig. Given the total volume of 930 mL (1L – 63 mL of liquefied PMDI, assuming a density close to 1 g/mL), we find 0.37 moles of gas in the headspace through the ideal gas law. Given the estimate for the headspace mass of gas of 23.5g, this equates to a molecular weight of 78

g/mol. This estimate is high given that we believe based on previous work at Sandia and elsewhere that the majority of evolved gas is CO_2 with a molecular weight of 44 g/mol (Erickson, 2006). The error in our molecular-weight estimate likely comes from inaccurate measurement of the mass of liquefied material due to material left behind in the pressure vessel, i.e. poor yield accuracy. This can be addressed in future work by using a removable sleeve within the pressure vessel.

Looking at Figure 8, the pressure during the cool down portion of the run is linear with R^2 = 0.9997, showing little deviation from ideal gas behavior, which implies that only a small portion of the evolved gas was condensable into the liquefied PMDI. This is an important result, as it justifies preparing liquefied materials in one vessel, cooling it to room temperature, and then transferring it to other instruments for further analysis.

3.1.2 Composition of the Decomposed PMDI foam

Table 1. Liquefied PMDI composition

Peak Name	CAS No.	Rel. Area	Probability	Retention Time (min)
Aniline	62-53-3	39.94	74	6.405
p-Aminotoluene	106-49-0	19.73	72	9.723
Propylene Glycol	57-55-6	11.32	80	1.535
Methcathinone	5650-44-2	6.24	38	0.775
2-Pentanone, 4-hydroxy-4-methyl	123-42-2	3.89	73	0.574
Benzenemethanol, .alpha.-(ethox	22383-53-5	2.51	75	9.733
2-Propanol, 1,1'-[(1-methyl-1,2	1638-16-0	2.49	93	9.183
2-Propanol, 1,1'-[(1-methyl-1,2	1638-16-0	2.15	99	17.549
Benzenamine, 2,5-dimethyl-	95-78-3	1.44	41	12.192
1,2-Diphenylethylamine	25611-78-3	0.89	89	14.422
Dodecane	112-40-3	0.87	34	13.935
Benzenamine, N,3-dimethyl-	696-44-6	0.74	53	12.461
1,2-Diphenylethylamine	25611-78-3	0.68	71	14.766
2-Propanol, 1,1'-[(1-methyl-1,2	1638-16-0	0.66	89	11.035
Benzenamine, 2-ethyl-6-methyl-	24549-06-2	0.65	94	15.314
Pyridine, 3-methyl-	108-99-6	0.63	36	6.007
3,3'-Diaminodiphenylmethane	19471-12-6	0.61	79	33.34
1H-Indole, 7-methyl-	933-67-5	0.60	70	18.89
1H-Indole, 3-methyl-	83-34-1	0.49	61	18.82
1,2-Diphenylethylamine	25611-78-3	0.43	76	15.45
N-(2-Hydroxyethyl)-N-methylanil	93-90-3	0.38	90	19.235
Pyridine, 3-ethyl-4-methyl-	529-21-5	0.34	83	11.431
Benzenamine, 4,4'-methylenebis-	101-77-9	0.33	93	34.615
1,2-Diphenylethylamine	25611-78-3	0.29	66	19.525
Quinoline	91-22-5	0.28	64	14.602
Benzeneacetonitrile, 2-cyano-	3759-28-2	0.26	90	17.987
Isoquinoline, 1-methyl-	1721-93-3	0.25	55	16.637
Diphenylamine	122-39-4	0.22	61	24.532
Diisooctyl adipate	1330-86-5	0.16	58	0.228
2-Fluorenamine	153-78-6	0.16	70	29.685
Propane, 1,1'-[ethylidenebis(ox	105-82-8	0.12	86	2.625
Indole	120-72-9	0.12	77	16.322
Acridine, 9,10-dihydro-9,9-dime	2-3-6267	0.09	99	31.843
Benzene, 1-ethyl-3-methyl-	620-14-4	0.05	32	5.826
Hexanedioic acid, dioctyl ester	123-79-5	0.00	64	0.465

Gas Chromatograph Mass Spectrometry (GC/MS) results of samples of the liquefied 20lb/ft^3 PMDI foam dissolved into acetone are shown in Table 1. We do not yet have quantitative information on concentrations of the above listed compounds, but aniline and polyols were a significant portion of the liquefied product, based on chromatograph peak area, which is consistent with the literature discussed in Section 1. This is an important result because aniline is reactive and may explain channeling and erosion behavior seen previously in some foam-in-a-can (FIC) tests, which we have not been able to observe with gas pressure alone (Section 3.4). Notice also that little CO_2 or other light hydrocarbons were observed, which implies that these compounds have a low solubility in the liquefied phase.

3.3 Rheology of liquefied PMDI foam

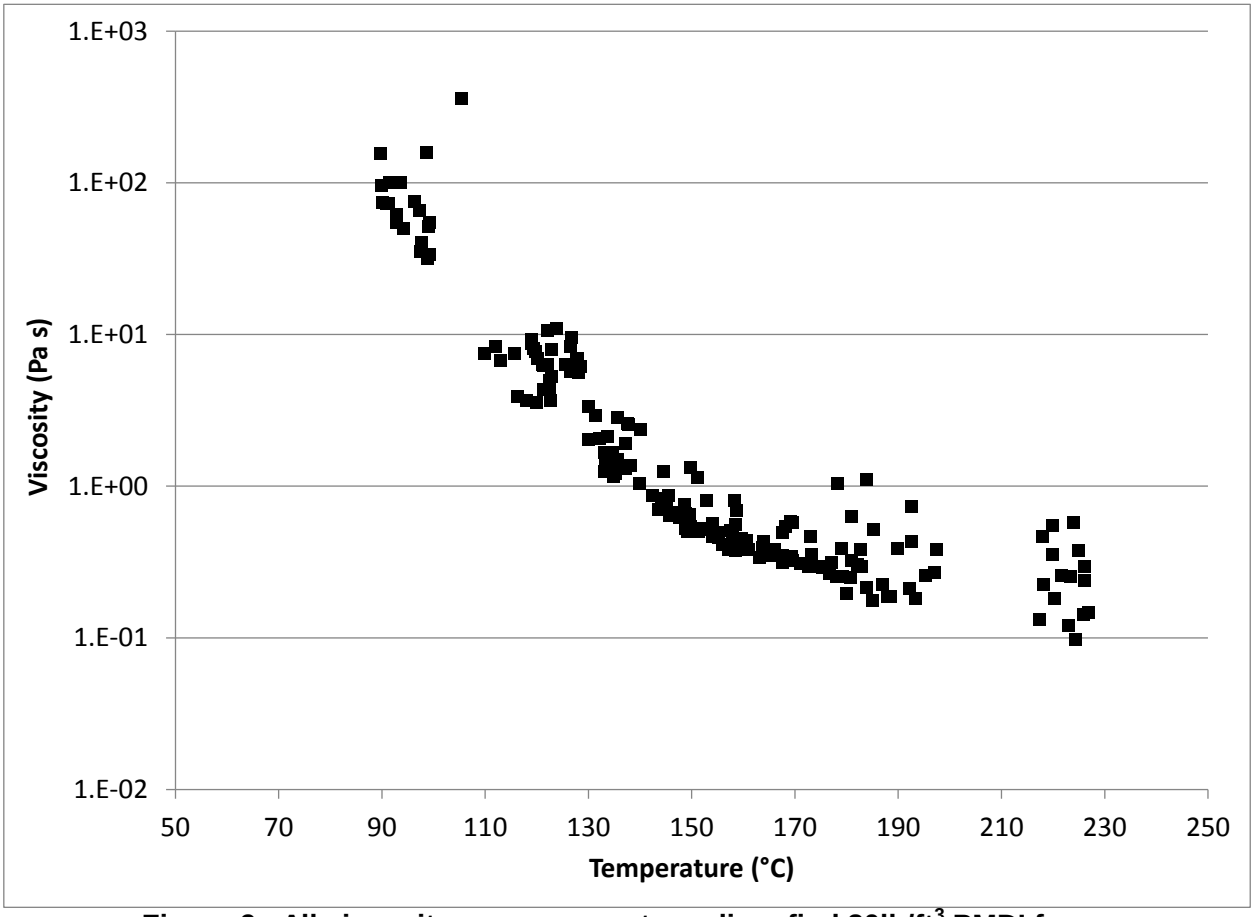

Figure 9. All viscosity measurements on liquefied 20lb/ft^3 PMDI foam.

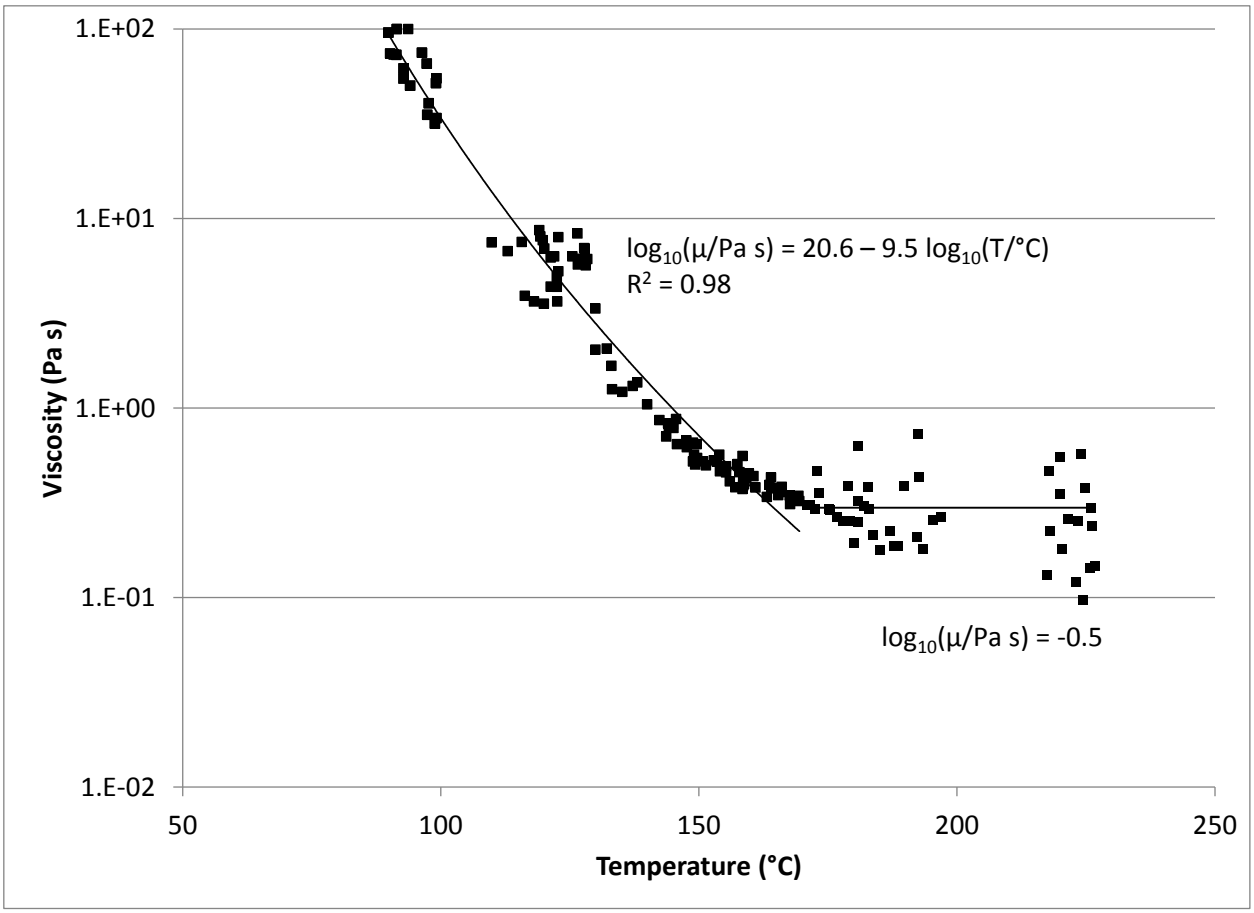

Figure 10. Filtered viscosity data and a possible fit.

Figure 9 shows all raw rheological measurements made on the 20lb/ft^3 PMDI foam from 90 °C to 230 °C. The data generally shows power law decay with increasing temperature until about 170 °C where the data starts to curve over towards 0.3 Pa s (100 centipoise or 100 times the viscosity of water); viscosity on the order of 0.1 Pa s is approaching the lower detection limit of the rheometer. Thus our estimate of 0.3 Pa s ($\log_{10} = -0.5$) for the viscosity of the liquefied PMDI at temperatures above 170 °C should be considered an upper bound.

The inner rotating cylinder on the rheometer makes physical contact with the inside of the upper lid of the pressure vessel via a millimeter-sized sapphire bearing. This bearing adds friction and causes the viscosity to vary with the inner-cylinder rotation rate even for Newtonian fluids. By increasing the rotation rate until the viscosity plateaus, one can remove the effect of the sapphire bearing. The data corresponding only to this plateau is shown in Figure 10. A fit is also given with a power law dependence on temperature for T < 170 °C, and constant viscosity for T > 170 °C. We leave it to the reader to decide how best to fit the data for future modeling efforts. The complete data is given in Appendix A.

The rheometer was checked against a Brookfield HT-30000 standard which has a known viscosity as a function of temperature (29.4 Pa s at 25 °C, 9.3 Pa s at 93 °C, and 4.6 Pa s at 149 °C). The check is given in Appendix A, the plateau effect of the sapphire bearing can be clearly seen in Figure 12, also given in Appendix A.

3.4 Mechanical Breakthrough of PMDI foam

Table 2. Mechanical breakthrough pressures of 10 and 20 lb/ft^3 PMDI foam

Weight (lb/ft^3)	Temp (°C)	Hold Time (min)[1]	Num. Tests	Breakthrough Pressure (psi)	Standard Deviation (psi)
10	80	20	8	286	45
10	80	10	8	241	78
10	180	5	8	171	21
10	180	20	8	180	19
10	120	5	8	228	28
10	120	10	8	267	42
20	80	5	8	322	40
20	80	20	8	894	62
20	120	20	8	750	110
20	120	10	8	723	135
20	180	20	8	636	88
20	180	10	8	535	136
20	180	5	4	561	141
20	80	10	8	740	181
20	80	5	8	817	203

1. The hold time in these tests is the time that the foam sample was held at a given temperature before beginning the mechanical test.

Table 2 shows the results of the experiments described in Section 2.4. The results indicate that 500 – 800 psi is required to initiate fracture through 20 lb/ft^3 PMDI foam and 170-300 psi is required for 10 lb/ft^3 PMDI foam. This is consistent with the permeameter experiments described in Section 3.5 on 20lb/ft^3 foam, which thus far have not shown breakthrough at pressures up to 500 psi.

3.5 Gas Breakthrough of PMDI foam

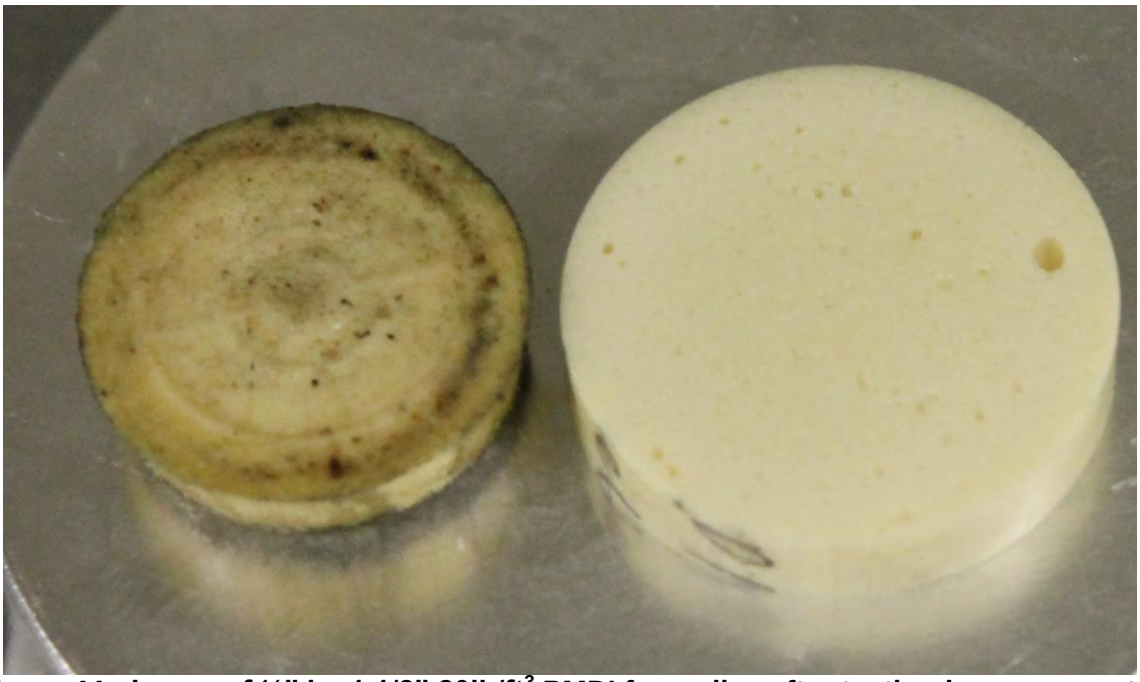

Figure 11. Image of ¼" by 1 1/8" 20lb/ft^3 PMDI foam disc after testing in permeameter (left) and an example piece before (right). The foam was heated in the permeameter to 200 °C, with a confining pressure of 300 psi and a driving pressure of 100 psi.

Only initial experimental observations will be reported here on the permeability studies of PMDI foam. Thus far we have not been able to observe gas penetrate 20lb/ft^3 PMDI foam. As one can ascertain from Table 2, for 20lb/ft^3 PMDI foam, at temperatures approaching 200 °C, we need pressures of at least 500 psi to cause rupture. Furthermore in these studies we applied a confining pressure to prevent gas from flowing around the sample. Because the temperature was above the glass transition point of the foam (T_g ~ 180 °C), the foam was able to compress (Figure 11) which may have caused the foam to become more resistant to penetration. Future work will examine lower density foams, and higher pressures with/without confining stresses.

3. CONCLUSIONS

A study was presented herein demonstrating that PMDI foam can be liquefied without appreciable losses of volatile organics. Further it has been demonstrated that it is possible to obtain rheological data on liquefied organic materials by confining them within a HTHP rheometer vessel. Mechanical tests were performed to determine the mechanical pressure required to penetrate into the foam. These tests are a precursor to future permeability experiments.

Because the mechanical pressures required to penetrate the foam were high compared with observations from FIC tests, and because of the significant amounts of aniline in the liquefied material, we have reason to believe that chemical rather than mechanical attack may be responsible for channeling and erosion seen in FIC tests. Thus, future work will include determining the ability of the liquefied foam to chemically erode through the foam. Other future work includes thermal conductivity and heat capacity of the liquefied PMDI material, vapor pressure as a function of mass loss, and eventually a repeat of these experiments on TDI.

4. REFERENCES

Allan, D., J. Daly, and J. J. Liggat. "Thermal volatilisation analysis of TDI-based flexible polyurethane foam." [In English]. *Polymer Degradation and Stability* 98, No. 2 (Feb 2013): 535-41. 10.1016/j.polymdegradstab.2012.12.002.

Bilbao, R., J. F. Mastral, J. Ceamanos, and M. E. Aldea. "Kinetics of the thermal decomposition of polyurethane foams in nitrogen and air atmospheres." [In English]. *Journal of Analytical and Applied Pyrolysis* 37, No. 1 (Aug 1996): 69-82. 10.1016/0165-2370(96)00936-9.

Chattopadhyay, D. K., and D. C. Webster. "Thermal stability and flame retardancy of polyurethanes." [In English]. *Progress in Polymer Science* 34, No. 10 (Oct 2009): 1068-133. 10.1016/j.progpolymsci.2009.06.002.

Erickson, K. L. "Thermal Decomposition Mechanisms Associated with Functional Groups in Selected Polymers." Paper presented at the 2006 NATAS Conference, Bowling Green, KY, 2006. SAND2006-3666C.

Erickson, K. L. "Thermal decomposition mechanisms common to polyurethane, epoxy, poly(diallyl phthalate), polycarbonate and poly(phenylene sulfide)." [In English]. *Journal of Thermal Analysis and Calorimetry* 89, No. 2 (Aug 2007): 427-40. 10.1007/s10973-006-8218-6.

Hentschel, T., and H. Munstedt. "Kinetics of the molar mass decrease in a polyurethane melt: a rheological study." [In English]. *Polymer* 42, No. 7 (Mar 2001): 3195-203. 10.1016/s0032-3861(00)00489-4.

Herrera, M., G. Matuschek, and A. Kettrup. "Thermal degradation of thermoplastic polyurethane elastomers (TPU) based on MDI." [In English]. *Polymer Degradation and Stability* 78, No. 2 (Nov 2002): 323-31. 10.1016/s0141-3910(02)00181-7.

Hobbs, M. L., K. L. Erickson, and T. Y. Chu, *Modeling decomposition of unconfined rigid polyurethane foam*, Sandia National Laboratories, Albuquerque, NM, 1999. SAND99-2758

Hobbs, M. L., K. L. Erickson, T. Y. Chu, T. T. I. Borek, A. M. Renlund, D. J. Clayton, and T. H. Fletcher. "Fire-induced response in polyurethane foam encapsulants." Paper presented at the Twenty-Ninth International Symposium on Combustion Japan, 2001a. SAND2001-3844C.

Hobbs, M. L., K. L. Erickson, T. Y. Chu, T. H. Fletcher, and D. J. Clayton. "Decomposition of rigid, closed-cell polyurethane foam." Paper presented at the ICCE/8, Tenerife, Spain, 2001b. SAND2001-1454C.

Jiao, L. L., H. H. Xiao, Q. S. Wang, and J. H. Sun. "Thermal degradation characteristics of rigid polyurethane foam and the volatile products analysis with TG-FTIR-MS." [In English]. *Polymer Degradation and Stability* 98, No. 12 (Dec 2013): 2687-96. 10.1016/j.polymdegradstab.2013.09.032.

Kim, B. H., K. Yoon, and D. C. Moon. "Thermal degradation behavior of rigid and soft polyurethanes based on methylene diphenyl diisocyanate using evolved gas analysis-(gas chromatography)-mass spectrometry." [In English]. *Journal of Analytical and Applied Pyrolysis* 98 (Nov 2012): 236-41. 10.1016/j.jaap.2012.09.010.

Li, S., J. Zhi, K. Yuan, and S. Yu. "Studies on the Thermal Behavior of Polyurethanes." *Polymer-Plastics Technology and Engineering* 45 (2006): 95-108.

Pfeiffer, J., and E. Steger. "Identification by infrared spectroscopy of thermal decomposition products of PVC and rigid polyurethane foam." [In German]. *Plaste und Kautschuk* 25, No. 8 (Aug. 1978): 459-62.

Wang, S., H. Chen, and L. Zhang. "Thermal Decomposition Kinetics of Rigid Polyurethane Foam and Ignition Risk by a Hot Particle." *Journal of Applied Polymer Science* (2014). DOI: 10.1002/APP.39359.

Yang, W. P., C. W. Macosko, and S. T. Wellinghoff. "THERMAL-DEGRADATION OF URETHANES BASED ON 4,4'-DIPHENYLMETHANE DIISOCYANATE AND 1,4-BUTANEDIOL (MDI/BDO)." [In English]. *Polymer* 27, No. 8 (Aug 1986): 1235-40. 10.1016/0032-3861(86)90012-1.

APPENDIX A: VISCOSITY RAW DATA

Table 3. Raw Rheological data from 20lb/ft^3 PMDI decomposed on 1/17/2013.

Temperature ºC	Stress Pa	Shear rate 1/s	Viscosity Pa s	Torque Nm
89.7	1.87E+01	1.21E-01	1.55E+02	7.80E-04
89.7	1.87E+01	1.21E-01	1.55E+02	7.80E-04
89.9	3.51E+01	3.66E-01	9.59E+01	1.46E-03
89.9	3.51E+01	3.66E-01	9.59E+01	1.46E-03
90.2	6.58E+01	8.88E-01	7.41E+01	2.74E-03
90.2	6.58E+01	8.88E-01	7.41E+01	2.74E-03
90.9	6.58E+01	8.97E-01	7.33E+01	2.74E-03
90.9	6.58E+01	8.97E-01	7.33E+01	2.74E-03
91.4	4.33E+01	5.94E-01	7.29E+01	1.80E-03
91.4	4.33E+01	5.94E-01	7.29E+01	1.80E-03
91.5	3.51E+01	3.52E-01	9.99E+01	1.46E-03
91.5	3.51E+01	3.52E-01	9.99E+01	1.46E-03
92.8	8.11E+01	1.48E+00	5.47E+01	3.38E-03
92.8	4.33E+01	6.99E-01	6.19E+01	1.80E-03
92.8	8.11E+01	1.48E+00	5.47E+01	3.38E-03
92.8	4.33E+01	6.99E-01	6.19E+01	1.80E-03
93.7	1.87E+01	1.88E-01	9.99E+01	7.80E-04
93.7	1.87E+01	1.88E-01	9.99E+01	7.80E-04
94.1	8.11E+01	1.61E+00	5.02E+01	3.38E-03
94.1	8.11E+01	1.61E+00	5.02E+01	3.38E-03
96.4	2.31E+01	3.09E-01	7.49E+01	9.62E-04
96.4	2.31E+01	3.09E-01	7.49E+01	9.62E-04
97.3	2.31E+01	3.52E-01	6.56E+01	9.62E-04
97.3	2.31E+01	3.52E-01	6.56E+01	9.62E-04
97.4	1.00E+02	2.84E+00	3.53E+01	4.16E-03
97.4	1.00E+02	2.84E+00	3.53E+01	4.16E-03
97.7	5.34E+01	1.32E+00	4.06E+01	2.22E-03
97.7	5.34E+01	1.32E+00	4.06E+01	2.22E-03
98.7	1.52E+01	9.60E-02	1.58E+02	6.32E-04
98.7	1.52E+01	9.60E-02	1.58E+02	6.32E-04
98.9	1.00E+02	3.16E+00	3.17E+01	4.16E-03
98.9	1.00E+02	3.16E+00	3.17E+01	4.16E-03
99.1	2.85E+01	5.49E-01	5.18E+01	1.19E-03
99.1	2.85E+01	5.49E-01	5.18E+01	1.19E-03
99.2	5.34E+01	1.58E+00	3.38E+01	2.22E-03
99.2	2.85E+01	5.19E-01	5.49E+01	1.19E-03
99.2	5.34E+01	1.58E+00	3.38E+01	2.22E-03

99.2	2.85E+01	5.19E-01	5.49E+01	1.19E-03
105.4	3.00E+01	8.36E-02	3.59E+02	1.92E-03
109.9	8.25E+01	1.10E+01	7.47E+00	5.28E-03
112.1	8.00E+01	9.63E+00	8.31E+00	3.33E-03
113	6.50E+01	9.66E+00	6.73E+00	4.16E-03
115.7	4.75E+01	6.33E+00	7.51E+00	3.04E-03
116.3	1.00E+02	2.56E+01	3.91E+00	6.40E-03
118.1	8.25E+01	2.26E+01	3.65E+00	5.28E-03
119.1	3.00E+01	3.26E+00	9.21E+00	1.92E-03
119.1	1.90E+01	2.18E+00	8.68E+00	7.89E-04
119.3	1.84E+01	2.30E+00	8.03E+00	7.67E-04
119.8	1.95E+01	2.54E+00	7.67E+00	8.11E-04
120	6.50E+01	1.83E+01	3.55E+00	4.16E-03
120.1	1.90E+01	2.73E+00	6.94E+00	7.89E-04
121.1	4.75E+01	7.45E+00	6.38E+00	3.04E-03
121.3	1.00E+02	2.29E+01	4.36E+00	6.40E-03
121.3	1.95E+01	3.13E+00	6.22E+00	8.11E-04
122	2.00E+01	3.17E+00	6.30E+00	8.33E-04
122.1	1.53E+01	1.43E+00	1.07E+01	6.35E-04
122.5	6.50E+01	1.32E+01	4.93E+00	4.16E-03
122.5	8.25E+01	1.90E+01	4.35E+00	5.28E-03
122.6	4.75E+01	1.30E+01	3.65E+00	3.04E-03
122.8	2.00E+01	3.80E+00	5.27E+00	8.33E-04
122.8	1.79E+01	2.25E+00	7.96E+00	7.45E-04
123.9	1.58E+01	1.44E+00	1.10E+01	6.57E-04
125.5	1.74E+01	2.76E+00	6.31E+00	7.23E-04
126.5	1.63E+01	1.96E+00	8.35E+00	6.79E-04
126.6	1.84E+01	3.22E+00	5.72E+00	7.67E-04
126.8	1.58E+01	1.66E+00	9.49E+00	6.57E-04
127.2	1.68E+01	2.75E+00	6.13E+00	7.01E-04
127.8	1.68E+01	2.42E+00	6.97E+00	7.01E-04
127.9	1.63E+01	2.35E+00	6.94E+00	6.79E-04
128.1	1.79E+01	3.16E+00	5.66E+00	7.45E-04
128.4	1.74E+01	2.84E+00	6.12E+00	7.23E-04
130	1.00E+02	4.92E+01	2.03E+00	6.40E-03
130	3.00E+01	8.96E+00	3.35E+00	1.92E-03
131.3	3.00E+01	1.03E+01	2.92E+00	1.25E-03
132.2	4.00E+01	1.95E+01	2.06E+00	1.67E-03
133.1	5.00E+01	3.00E+01	1.67E+00	2.08E-03
133.2	8.25E+01	6.57E+01	1.26E+00	5.28E-03
133.3	5.00E+01	3.30E+01	1.51E+00	3.20E-03
133.4	6.50E+01	4.66E+01	1.40E+00	4.16E-03
133.6	6.50E+01	4.76E+01	1.37E+00	4.16E-03

133.7	5.00E+01	3.16E+01	1.58E+00	3.20E-03
133.8	4.00E+01	1.90E+01	2.11E+00	2.56E-03
134.6	4.00E+01	2.38E+01	1.68E+00	2.56E-03
134.8	1.00E+02	8.58E+01	1.17E+00	6.40E-03
135.2	6.50E+01	5.35E+01	1.22E+00	4.16E-03
135.4	4.75E+01	3.30E+01	1.44E+00	3.04E-03
135.6	3.00E+01	1.06E+01	2.82E+00	1.92E-03
135.7	4.75E+01	3.19E+01	1.49E+00	3.04E-03
137.1	3.00E+01	1.56E+01	1.92E+00	1.25E-03
137.2	4.75E+01	3.64E+01	1.31E+00	3.04E-03
137.6	3.00E+01	1.16E+01	2.58E+00	1.92E-03
137.8	3.00E+01	1.17E+01	2.56E+00	1.92E-03
138.1	4.00E+01	2.94E+01	1.36E+00	1.67E-03
140	5.00E+01	4.78E+01	1.05E+00	2.08E-03
140.1	3.00E+01	1.28E+01	2.35E+00	1.92E-03
142.4	9.00E+01	1.04E+02	8.63E-01	5.76E-03
143.7	1.00E+02	1.42E+02	7.07E-01	6.40E-03
144.1	1.00E+02	1.21E+02	8.28E-01	6.40E-03
144.1	8.00E+01	9.64E+01	8.30E-01	5.12E-03
144.2	8.25E+01	1.03E+02	8.03E-01	5.28E-03
144.3	1.00E+02	1.27E+02	7.84E-01	6.40E-03
144.6	3.00E+01	2.42E+01	1.24E+00	1.25E-03
144.7	8.25E+01	1.00E+02	8.25E-01	5.28E-03
144.8	6.00E+01	7.24E+01	8.29E-01	3.84E-03
145	7.00E+01	8.56E+01	8.18E-01	4.48E-03
145.1	1.00E+02	1.28E+02	7.84E-01	6.40E-03
145.6	4.00E+01	4.58E+01	8.74E-01	1.67E-03
145.8	8.40E+01	1.31E+02	6.44E-01	5.37E-03
147.6	5.00E+01	7.41E+01	6.75E-01	2.08E-03
147.7	6.80E+01	1.10E+02	6.20E-01	4.35E-03
148.6	3.00E+01	3.95E+01	7.59E-01	1.25E-03
148.9	1.00E+02	1.92E+02	5.22E-01	4.16E-03
148.9	4.00E+01	6.10E+01	6.56E-01	1.67E-03
149.1	5.00E+01	8.81E+01	5.67E-01	2.08E-03
149.3	9.00E+01	1.79E+02	5.04E-01	3.75E-03
149.6	5.20E+01	8.06E+01	6.45E-01	3.33E-03
149.7	7.00E+01	1.29E+02	5.45E-01	2.91E-03
149.8	2.00E+01	1.50E+01	1.33E+00	8.33E-04
150.8	1.00E+02	1.91E+02	5.23E-01	6.40E-03
151.1	3.60E+01	3.15E+01	1.14E+00	2.30E-03
151.4	8.00E+01	1.61E+02	4.98E-01	3.33E-03
152.8	3.00E+01	3.75E+01	8.01E-01	1.25E-03
152.9	8.40E+01	1.59E+02	5.29E-01	5.37E-03

153.5	5.00E+01	9.60E+01	5.21E-01	2.08E-03
154	4.00E+01	7.06E+01	5.67E-01	1.67E-03
154.1	6.00E+01	1.30E+02	4.63E-01	2.50E-03
155.3	6.80E+01	1.38E+02	4.93E-01	4.35E-03
155.3	5.00E+01	1.09E+02	4.57E-01	2.08E-03
156	1.00E+02	2.44E+02	4.10E-01	4.16E-03
157.1	7.00E+01	1.84E+02	3.82E-01	2.91E-03
157.5	5.20E+01	1.03E+02	5.06E-01	3.33E-03
157.9	4.00E+01	8.74E+01	4.58E-01	1.67E-03
158.4	2.00E+01	2.51E+01	7.98E-01	8.33E-04
158.5	9.00E+01	2.41E+02	3.73E-01	3.75E-03
158.5	3.00E+01	5.37E+01	5.58E-01	1.25E-03
158.6	1.00E+02	2.45E+02	4.08E-01	6.40E-03
158.6	8.00E+01	2.05E+02	3.90E-01	3.33E-03
158.8	3.60E+01	5.18E+01	6.95E-01	2.30E-03
158.8	6.00E+01	1.52E+02	3.96E-01	2.50E-03
159.2	1.00E+02	2.36E+02	4.25E-01	6.40E-03
159.7	8.40E+01	1.86E+02	4.51E-01	5.37E-03
160.6	1.00E+02	2.29E+02	4.38E-01	6.40E-03
161	8.40E+01	2.21E+02	3.80E-01	5.37E-03
163.2	8.40E+01	2.48E+02	3.39E-01	5.37E-03
163.7	6.80E+01	1.73E+02	3.93E-01	4.35E-03
164	1.00E+02	2.33E+02	4.30E-01	6.40E-03
164.1	6.80E+01	1.81E+02	3.77E-01	4.35E-03
165.4	6.80E+01	1.96E+02	3.47E-01	4.35E-03
165.7	8.40E+01	2.34E+02	3.59E-01	5.37E-03
165.9	5.20E+01	1.37E+02	3.79E-01	3.33E-03
166.1	5.20E+01	1.35E+02	3.84E-01	3.33E-03
167.6	3.60E+01	7.28E+01	4.95E-01	2.30E-03
167.6	6.80E+01	1.97E+02	3.46E-01	4.35E-03
167.7	5.50E+01	1.77E+02	3.11E-01	3.52E-03
168.1	5.20E+01	1.54E+02	3.38E-01	3.33E-03
168.1	3.60E+01	6.69E+01	5.38E-01	2.30E-03
169.2	3.60E+01	6.12E+01	5.88E-01	2.30E-03
169.3	5.20E+01	1.51E+02	3.44E-01	3.33E-03
169.5	3.60E+01	6.26E+01	5.75E-01	2.30E-03
169.5	7.50E+01	2.32E+02	3.23E-01	4.80E-03
171	5.10E+01	1.65E+02	3.09E-01	3.26E-03
171.6	7.50E+01	2.43E+02	3.09E-01	4.80E-03
172.6	4.50E+01	1.54E+02	2.93E-01	2.88E-03
173	8.40E+01	1.82E+02	4.62E-01	5.37E-03
173.3	3.60E+01	1.02E+02	3.54E-01	2.30E-03
175.2	3.90E+01	1.33E+02	2.93E-01	2.50E-03

175.4	6.80E+01	2.34E+02	2.91E-01	4.35E-03
176.7	6.50E+01	2.43E+02	2.67E-01	4.16E-03
177.1	3.50E+01	1.11E+02	3.15E-01	2.24E-03
178	5.20E+01	2.04E+02	2.55E-01	3.33E-03
178.2	1.00E+02	9.56E+01	1.05E+00	6.40E-03
179	7.50E+01	1.94E+02	3.87E-01	4.80E-03
179.2	6.30E+01	2.50E+02	2.52E-01	4.03E-03
180	5.00E+01	2.57E+02	1.95E-01	2.08E-03
180.8	3.67E+01	1.47E+02	2.50E-01	1.53E-03
180.9	3.60E+01	1.12E+02	3.21E-01	2.30E-03
180.9	8.40E+01	1.34E+02	6.28E-01	5.37E-03
182.1	6.38E+01	2.10E+02	3.04E-01	4.08E-03
182.8	6.80E+01	1.78E+02	3.83E-01	4.35E-03
182.9	4.13E+01	1.41E+02	2.93E-01	2.64E-03
183.8	5.20E+01	2.44E+02	2.13E-01	3.33E-03
183.9	1.00E+02	9.05E+01	1.11E+00	6.40E-03
185.1	4.56E+01	2.57E+02	1.77E-01	1.90E-03
185.3	3.00E+01	5.76E+01	5.21E-01	1.92E-03
187	5.25E+01	2.35E+02	2.23E-01	3.36E-03
187.9	4.11E+01	2.21E+02	1.86E-01	1.71E-03
188.5	4.40E+01	2.36E+02	1.86E-01	2.82E-03
189.8	3.00E+01	7.71E+01	3.89E-01	1.92E-03
192.3	3.60E+01	1.72E+02	2.09E-01	2.30E-03
192.5	7.50E+01	1.03E+02	7.30E-01	4.80E-03
192.6	6.38E+01	1.48E+02	4.32E-01	4.08E-03
193.4	4.13E+01	2.28E+02	1.81E-01	2.64E-03
195.4	5.20E+01	2.02E+02	2.58E-01	3.33E-03
197	5.25E+01	1.96E+02	2.68E-01	3.36E-03
197.4	6.00E+01	1.56E+02	3.84E-01	3.84E-03
217.4	2.78E+01	2.11E+02	1.31E-01	1.16E-03
217.9	4.56E+01	9.83E+01	4.64E-01	1.90E-03
218.1	3.22E+01	1.44E+02	2.24E-01	1.34E-03
220	3.67E+01	1.04E+02	3.52E-01	1.53E-03
220	4.11E+01	7.45E+01	5.52E-01	1.71E-03
220.3	1.89E+01	1.04E+02	1.81E-01	7.86E-04
221.6	5.00E+01	1.93E+02	2.59E-01	2.08E-03
223.1	2.33E+01	1.94E+02	1.20E-01	9.71E-04
223.4	5.00E+01	1.96E+02	2.55E-01	2.08E-03
224	4.11E+01	7.16E+01	5.75E-01	1.71E-03
224.4	2.33E+01	2.40E+02	9.73E-02	9.71E-04
224.9	3.67E+01	9.69E+01	3.79E-01	1.53E-03
225.9	1.89E+01	1.32E+02	1.43E-01	7.86E-04
226	4.56E+01	1.55E+02	2.95E-01	1.90E-03

226.1	3.22E+01	1.35E+02	2.39E-01	1.34E-03
226.8	2.78E+01	1.90E+02	1.46E-01	1.16E-03

Table 4. Measured viscosity of Brookfield HT-30000 standard

Temperature °C	Stress Pa	Shear rate 1/s	Viscosity Pa s	Torque Nm
101.1	5.00E+01	2.80E+00	1.79E+01	3.20E-03
100.9	5.67E+01	3.78E+00	1.50E+01	3.63E-03
100.6	6.33E+01	4.72E+00	1.34E+01	4.05E-03
100.3	7.00E+01	5.60E+00	1.25E+01	4.48E-03
100.2	7.67E+01	6.44E+00	1.19E+01	4.91E-03
100.1	8.33E+01	7.09E+00	1.18E+01	5.33E-03
100	9.00E+01	7.79E+00	1.16E+01	5.76E-03
100	9.67E+01	7.60E+00	1.27E+01	6.19E-03
99.9	1.03E+02	8.45E+00	1.22E+01	6.61E-03
99.9	1.10E+02	9.04E+00	1.22E+01	7.04E-03
100	5.00E+01	2.78E+00	1.80E+01	3.20E-03
100	5.67E+01	3.84E+00	1.48E+01	3.63E-03
100.1	6.33E+01	4.65E+00	1.36E+01	4.05E-03
100.1	7.00E+01	5.45E+00	1.28E+01	4.48E-03
100	7.67E+01	6.13E+00	1.25E+01	4.91E-03
100	8.33E+01	6.70E+00	1.24E+01	5.33E-03
100.1	9.00E+01	7.34E+00	1.23E+01	5.76E-03
100	9.67E+01	8.20E+00	1.18E+01	6.19E-03
100.1	1.03E+02	9.14E+00	1.13E+01	6.61E-03
100	1.10E+02	9.76E+00	1.13E+01	7.04E-03
100	5.00E+01	3.08E+00	1.63E+01	3.20E-03
100.1	5.67E+01	3.74E+00	1.51E+01	3.63E-03
100	6.33E+01	4.88E+00	1.30E+01	4.05E-03
100	7.00E+01	5.59E+00	1.25E+01	4.48E-03
100	7.67E+01	6.44E+00	1.19E+01	4.91E-03
100.1	8.33E+01	7.03E+00	1.19E+01	5.33E-03
99.9	9.00E+01	7.66E+00	1.18E+01	5.76E-03
100	9.67E+01	8.42E+00	1.15E+01	6.19E-03
100	1.03E+02	9.23E+00	1.12E+01	6.61E-03
99.9	1.10E+02	9.90E+00	1.11E+01	7.04E-03
99.9	5.00E+01	3.29E+00	1.52E+01	3.20E-03
99.9	5.67E+01	4.11E+00	1.38E+01	3.63E-03
100	6.33E+01	4.79E+00	1.32E+01	4.05E-03
100	7.00E+01	5.78E+00	1.21E+01	4.48E-03
100.1	7.67E+01	6.45E+00	1.19E+01	4.91E-03

100	8.33E+01	7.18E+00	1.16E+01	5.33E-03
100	9.00E+01	7.87E+00	1.14E+01	5.76E-03
100	9.67E+01	8.64E+00	1.12E+01	6.19E-03
100.1	1.03E+02	9.33E+00	1.11E+01	6.61E-03
100	1.10E+02	9.98E+00	1.10E+01	7.04E-03
100	5.00E+01	3.04E+00	1.64E+01	3.20E-03
100	5.67E+01	4.24E+00	1.34E+01	3.63E-03
100	5.00E+01	3.38E+00	1.48E+01	3.20E-03
100	6.11E+01	4.68E+00	1.31E+01	3.91E-03
100	7.22E+01	5.93E+00	1.22E+01	4.62E-03
100.1	8.33E+01	7.01E+00	1.19E+01	5.33E-03
100.1	9.44E+01	8.24E+00	1.15E+01	6.04E-03
100	1.06E+02	9.49E+00	1.11E+01	6.75E-03
100	1.17E+02	1.08E+01	1.08E+01	7.46E-03
100.1	1.28E+02	1.21E+01	1.05E+01	8.17E-03
99.9	1.39E+02	1.33E+01	1.04E+01	8.89E-03
100.1	6.00E+01	4.51E+00	1.33E+01	3.84E-03
100	6.89E+01	5.71E+00	1.21E+01	4.41E-03
100	7.78E+01	6.75E+00	1.15E+01	4.98E-03
100.1	8.67E+01	8.04E+00	1.08E+01	5.55E-03
100.1	9.56E+01	9.01E+00	1.06E+01	6.11E-03
99.9	1.04E+02	9.94E+00	1.05E+01	6.68E-03
100	1.13E+02	1.06E+01	1.07E+01	7.25E-03
100.1	1.22E+02	1.16E+01	1.06E+01	7.82E-03
100	1.31E+02	1.25E+01	1.05E+01	8.39E-03
99.9	1.40E+02	1.34E+01	1.04E+01	8.96E-03
99.9	6.00E+01	4.47E+00	1.34E+01	3.84E-03
99.9	6.89E+01	5.55E+00	1.24E+01	4.41E-03
99.9	7.78E+01	6.52E+00	1.19E+01	4.98E-03
100	8.67E+01	7.35E+00	1.18E+01	5.55E-03
100.1	9.56E+01	8.42E+00	1.14E+01	6.11E-03
100.1	1.04E+02	9.30E+00	1.12E+01	6.68E-03
100	1.13E+02	1.01E+01	1.12E+01	7.25E-03
100	1.22E+02	1.10E+01	1.11E+01	7.82E-03
100.1	1.31E+02	1.20E+01	1.10E+01	8.39E-03
100	1.40E+02	1.28E+01	1.09E+01	8.96E-03
100	6.00E+01	4.30E+00	1.40E+01	3.84E-03
100	6.89E+01	5.20E+00	1.32E+01	4.41E-03
99.9	7.78E+01	6.33E+00	1.23E+01	4.98E-03
100.1	8.67E+01	7.34E+00	1.18E+01	5.55E-03
100	9.56E+01	8.39E+00	1.14E+01	6.11E-03
99.9	1.04E+02	9.30E+00	1.12E+01	6.68E-03
100	1.13E+02	1.02E+01	1.11E+01	7.25E-03

100.1	1.22E+02	1.11E+01	1.10E+01	7.82E-03
100.1	1.31E+02	1.21E+01	1.08E+01	8.39E-03
99.9	1.40E+02	1.29E+01	1.08E+01	8.96E-03
60.7	6.00E+01	2.59E+00	2.32E+01	3.84E-03
60.1	6.64E+01	2.86E+00	2.32E+01	4.25E-03
60.1	7.29E+01	3.32E+00	2.20E+01	4.66E-03
60.3	7.93E+01	3.72E+00	2.13E+01	5.07E-03
60.1	8.57E+01	4.10E+00	2.09E+01	5.48E-03
60.5	9.21E+01	4.43E+00	2.08E+01	5.90E-03
60.2	9.86E+01	4.07E+00	2.42E+01	6.31E-03
60.5	1.05E+02	4.71E+00	2.23E+01	6.72E-03
60.6	1.11E+02	4.56E+00	2.44E+01	7.13E-03
60.4	1.18E+02	3.98E+00	2.96E+01	7.54E-03
60.9	1.24E+02	4.94E+00	2.51E+01	7.95E-03
60.6	1.31E+02	5.11E+00	2.56E+01	8.36E-03
60.9	1.37E+02	5.32E+00	2.58E+01	8.77E-03
60.7	1.44E+02	5.97E+00	2.41E+01	9.19E-03
61	1.00E+02	4.49E+00	2.23E+01	6.40E-03
60.6	1.11E+02	5.35E+00	2.08E+01	7.12E-03
60.9	1.23E+02	6.19E+00	1.98E+01	7.84E-03
60.9	1.34E+02	6.71E+00	2.00E+01	8.56E-03
60.5	1.45E+02	7.08E+00	2.05E+01	9.28E-03
60.9	1.00E+02	3.93E+00	2.54E+01	6.40E-03
60.6	1.11E+02	4.64E+00	2.40E+01	7.12E-03
60.7	1.23E+02	4.78E+00	2.56E+01	7.84E-03
152.3	6.00E+01	6.76E+00	8.87E+00	3.84E-03
153.8	7.75E+01	1.02E+01	7.58E+00	4.96E-03
153.4	9.50E+01	1.31E+01	7.26E+00	6.08E-03
152.3	1.13E+02	1.59E+01	7.07E+00	7.20E-03
150.7	6.00E+01	8.43E+00	7.12E+00	3.84E-03
150.6	7.75E+01	1.17E+01	6.62E+00	4.96E-03
150.4	9.50E+01	1.50E+01	6.34E+00	6.08E-03
150.3	1.13E+02	1.80E+01	6.25E+00	7.20E-03
150.3	1.30E+02	2.08E+01	6.26E+00	8.32E-03
150.1	6.00E+01	8.95E+00	6.71E+00	3.84E-03
150.1	7.75E+01	1.21E+01	6.39E+00	4.96E-03
150.2	6.00E+01	7.32E+00	8.20E+00	3.84E-03
150.2	6.00E+01	7.24E+00	8.29E+00	3.84E-03
150.1	7.75E+01	1.07E+01	7.27E+00	4.96E-03
150	9.50E+01	1.25E+01	7.60E+00	6.08E-03
149.9	6.00E+01	5.34E+00	1.12E+01	3.84E-03
150.1	5.22E+01	6.32E+00	8.26E+00	3.34E-03
150.1	6.44E+01	7.77E+00	8.29E+00	4.12E-03

150.1	7.67E+01	9.40E+00	8.16E+00	4.91E-03
150.1	8.89E+01	1.20E+01	7.44E+00	5.69E-03
150.1	1.01E+02	1.42E+01	7.12E+00	6.47E-03
150.1	1.13E+02	1.58E+01	7.15E+00	7.25E-03
150.1	1.26E+02	1.83E+01	6.84E+00	8.03E-03
150	1.38E+02	2.14E+01	6.44E+00	8.82E-03
150	9.00E+01	1.27E+01	7.10E+00	5.76E-03
150.1	9.44E+01	1.35E+01	6.98E+00	6.04E-03
150.1	9.89E+01	1.41E+01	7.01E+00	6.33E-03
150.1	1.03E+02	1.46E+01	7.07E+00	6.61E-03
150.1	1.08E+02	1.48E+01	7.26E+00	6.89E-03
150	1.12E+02	1.49E+01	7.52E+00	7.18E-03
150	1.17E+02	1.74E+01	6.72E+00	7.46E-03
150	1.21E+02	1.76E+01	6.90E+00	7.75E-03
150	1.26E+02	1.81E+01	6.95E+00	8.03E-03
150	1.30E+02	1.84E+01	7.07E+00	8.32E-03
150	9.00E+01	1.23E+01	7.29E+00	5.76E-03
150	9.44E+01	1.20E+01	7.87E+00	6.04E-03
150	9.89E+01	1.69E+01	5.85E+00	6.33E-03
150.1	1.03E+02	1.77E+01	5.83E+00	6.61E-03
150	1.08E+02	1.88E+01	5.72E+00	6.89E-03
150	1.12E+02	9.59E+00	1.17E+01	7.18E-03
150	1.17E+02	1.15E+01	1.02E+01	7.46E-03
150	7.00E+01	3.78E+00	1.85E+01	4.48E-03
150.1	7.67E+01	3.30E+00	2.32E+01	4.91E-03
150	8.33E+01	7.52E+00	1.11E+01	5.33E-03
150.1	9.00E+01	8.54E+00	1.05E+01	5.76E-03
150	9.67E+01	1.28E+01	7.54E+00	6.19E-03
150	1.03E+02	1.27E+01	8.13E+00	6.61E-03
150	1.10E+02	1.54E+01	7.16E+00	7.04E-03
150	1.17E+02	1.59E+01	7.31E+00	7.46E-03
149.9	1.23E+02	1.87E+01	6.60E+00	7.89E-03
150	1.30E+02	1.55E+01	8.37E+00	8.32E-03
129.6	7.75E+01	8.15E+00	9.51E+00	4.96E-03
129.7	9.50E+01	9.24E+00	1.03E+01	6.08E-03
129.9	1.13E+02	1.64E+01	6.88E+00	7.20E-03
129.9	1.30E+02	1.92E+01	6.77E+00	8.32E-03
129.9	6.00E+01	5.60E+00	1.07E+01	3.84E-03
129.9	7.75E+01	9.66E+00	8.03E+00	4.96E-03
130	9.50E+01	1.26E+01	7.54E+00	6.08E-03
130	1.13E+02	1.52E+01	7.40E+00	7.20E-03
130	1.30E+02	1.79E+01	7.27E+00	8.32E-03
130	7.50E+01	4.51E+00	1.66E+01	4.80E-03

130	8.11E+01	1.07E+01	7.55E+00	5.19E-03
130	8.72E+01	1.21E+01	7.20E+00	5.58E-03
130	9.33E+01	1.35E+01	6.94E+00	5.97E-03
130	9.94E+01	1.46E+01	6.83E+00	6.36E-03
130	1.06E+02	1.54E+01	6.86E+00	6.75E-03
129.9	1.12E+02	1.61E+01	6.92E+00	7.14E-03
130	1.18E+02	1.70E+01	6.92E+00	7.53E-03
130	1.24E+02	1.77E+01	6.99E+00	7.92E-03
130	1.30E+02	1.88E+01	6.93E+00	8.32E-03
129.9	7.50E+01	9.76E+00	7.69E+00	4.80E-03
130	8.11E+01	1.07E+01	7.55E+00	5.19E-03
130.1	8.72E+01	1.17E+01	7.44E+00	5.58E-03
130	9.33E+01	1.26E+01	7.42E+00	5.97E-03
130.1	9.94E+01	1.39E+01	7.16E+00	6.36E-03
130	1.06E+02	1.48E+01	7.11E+00	6.75E-03
130.1	1.12E+02	1.59E+01	7.04E+00	7.14E-03
130	1.18E+02	1.68E+01	7.01E+00	7.53E-03
130.1	1.24E+02	1.76E+01	7.03E+00	7.92E-03
130	1.30E+02	1.84E+01	7.06E+00	8.32E-03
110	7.50E+01	7.07E+00	1.06E+01	4.80E-03
109.9	8.11E+01	8.31E+00	9.76E+00	5.19E-03
110	8.72E+01	9.43E+00	9.25E+00	5.58E-03
110	9.33E+01	1.02E+01	9.15E+00	5.97E-03
110	9.94E+01	1.08E+01	9.19E+00	6.36E-03
109.9	1.06E+02	1.16E+01	9.07E+00	6.75E-03
110	1.12E+02	1.22E+01	9.12E+00	7.14E-03
110	1.18E+02	1.32E+01	8.95E+00	7.53E-03
110.1	1.24E+02	1.40E+01	8.84E+00	7.92E-03
109.9	1.30E+02	1.31E+01	9.91E+00	8.32E-03
109.9	7.50E+01	6.60E+00	1.14E+01	4.80E-03
110	8.11E+01	7.09E+00	1.14E+01	5.19E-03
110	8.72E+01	8.60E+00	1.01E+01	5.58E-03
110	9.33E+01	9.26E+00	1.01E+01	5.97E-03
110	9.94E+01	1.01E+01	9.85E+00	6.36E-03
110.1	1.06E+02	1.11E+01	9.53E+00	6.75E-03
110	1.12E+02	1.17E+01	9.54E+00	7.14E-03
109.9	1.18E+02	1.26E+01	9.37E+00	7.53E-03
110	1.24E+02	1.31E+01	9.42E+00	7.92E-03
110.1	1.30E+02	1.42E+01	9.18E+00	8.32E-03

Table 5. Nominal viscosity values of Brookfield HT-30000 standard

Temp °C	Viscosity Pa s
25	29.44
93.3	9.275
149	4.625

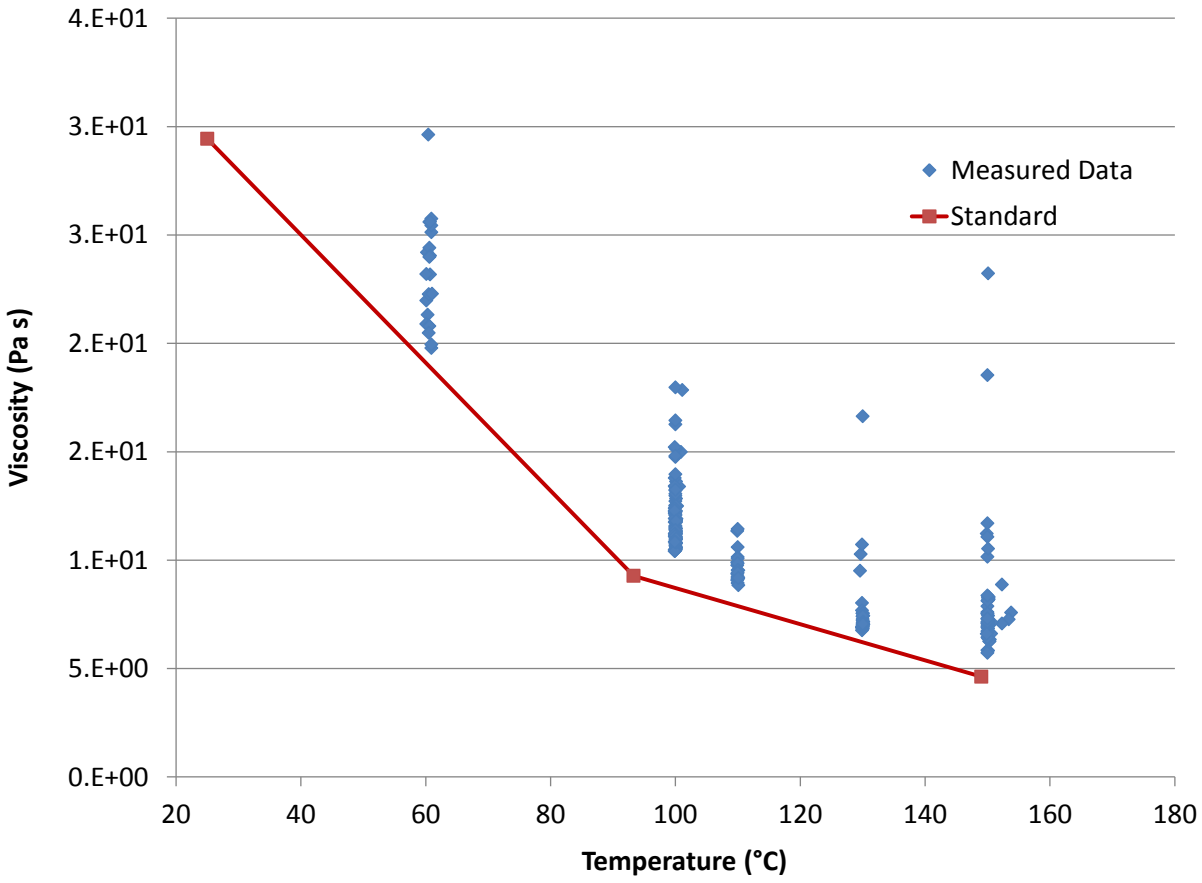

Figure 12. Measured versus nominal viscosity of Brookfield HT-30000 standard.

DISTRIBUTION (ELECTRONIC COPIES)

1	MS0346	Lisa A. Mondy	1512
1	MS0346	Christine C. Roberts	1512
1	MS0346	Anne M. Grillet	1512
1	MS0840	Kevin N. Long	1554
1	MS0888	Edward M. Russick	1833
1	MS0958	Haoran Deng	1833
1	MS0958	Lindsey G. Hughes	1835
1	MS1135	Randall D. Watkins	1532
1	MS9042	Sarah N. Scott	8365
1	MS9042	Amanda B. Dodd	8365
1	MS9403	LeRoy Whinnery	8223
1	MS9957	Ryan M. Keedy	8365
1	MS9957	Victor Brunini	8365
1	MS0899	Technical Library	9536 (electronic copy)


Sandia National Laboratories